



#### Available online at www.sciencedirect.com

# **ScienceDirect**

Procedia Manufacturing 37 (2019) 529-536



www.elsevier.com/locate/procedia

9th International Conference on Physical and Numerical Simulation of Materials Processing (ICPNS'2019)

# Parameters prediction of hot-pressing sintering of high entropy alloys using numerical modeling and simulation

Danni Yang<sup>a</sup>, Haopeng Jiang<sup>a</sup>, Yong Liu<sup>a,b</sup>, Zhonghong Lai<sup>a,c</sup>, Mingqing Liao<sup>a</sup>, Nan Qu<sup>a</sup>, Yitan Han<sup>a</sup>, Jingchuan Zhu<sup>a,b</sup>\*

<sup>a</sup> School of Materials Science and Engineering, Harbin Institute of Technology, Harbin 150001, Heilongjiang, China
 <sup>b</sup> National Key Laboratory for Precision Hot Processing of Metals, Harbin Institute of Technology, Harbin 150001, Heilongjiang, China
 <sup>c</sup> The Centre of Analysis Measurement, Harbin Institute of Technology, Harbin 150001, Heilongjiang, China

#### Abstract

In this work, numerical modeling and simulation method was firstly used to obtain the hot-pressing sintering parameter of high entropy alloy (HEA). The finite element model was built to describe the consolidation process. Constitutive relation of powder material was applied assuming that metal powder is a kind of elasto-plastic material with an elliptical yield criterion. The change law of relative density for sintered bulk varying with pressure, time and temperature were obtained. Besides, the flow stress as well as relative density distributions were acknowledged with different sintering time. The simulation results indicate that the HEA would achieve a relative density of more than 95 % if the pressure above 45 MPa at 1150 °C. The relative density from experiment is well agreement with that of simulation results when the sintering parameter are within the predicted range. This work is of great importance to the study of hot-press sintering of HEA.

© 2019 The Authors. Published by Elsevier B.V.

This is an open access article under the CC BY-NC-ND license (http://creativecommons.org/licenses/by-nc-nd/4.0/)
Peer-review under responsibility of the scientific committee of the 9th International Conference on Physical and Numerical Simulation on Materials Processing

Keywords: high entropy alloy; parameter prediction; hot-pressing sintering; numerical modeling and simulation

<sup>\*</sup> Corresponding author. Tel.: +86-0451-86402890. *E-mail address*: fgms@hit.edu.cn

#### 1. Introduction

High entropy alloys was proposed by Yeh et al. in 2004[1], these new series of alloy is consisted of at least four principal elements, and atomic concentration of each element ranges from 5% to 35 at. %. The effect of high entropy of multi-principal elements can give rise to severe lattice distortion and sluggish diffusion [2] comparing with that of conventional counterparts. And this new generation alloy provides a promising direction in metal development for excellent properties, such as high strength and hardness [3], understanding wear resistance [4], distinctive electrical and magnetic properties [5], etc., consequently, they are suitable for a wide range of industrial application.

The main method of preparing bulk alloys keeps arc-melting at present, however, the major disadvantage of this kind of processing method would cause dendritic microstructure together with selective segregation of the alloying element in the course of solidification, and a further step of heat treatment is needed [6]. Mechanically alloying (MA) and sintering, as a type of solid state processing route, has been widely used to prepare uniform microstructure and compositional homogeneity [7]. However, current studies of sintering parameter about high entropy alloys are based on empirical data, which limit a better understanding of this very complex process. In such case, numerical modeling and simulation is of great importance to the distribution of variables of stress and relative density [8]. Moreover, it give a possible way to search ideal parameter.

To perform numerical modeling, finite element modeling (FEM) is utilized combining with an appropriate constitutive relationship which can represent the properties and deformation behaviors of the powder. In this model of FEM, the powder is regarded as a continuum media, which is a kind of time-independent, elasto-plastic as well as compressible material. Moreover, the flow in porous body is regarded as depending on the hydrostatic stress. In the current work, the constitutive model of elliptical yield criterion has been used to describe the deformation behavior of MA-powder system during sintering process. Two dimensional model has been built, and we supposed that temperature is a function of time. Moreover, releasing of lattice stress and growth of grain size would occur due to the addition of temperature field. Also a sintering parameter for a certain relative density was obtained to guide the following experiment.

# 2. Material and method

# 2.1. Material

High purity Fe(>99.5wt%), Cr(>99.5wt%), Ni(>99.9wt%), Al(>99.5wt%) and Ti(>99wt%) powders were used to synthesize high entropy alloy (HEA) via mechanically alloying (MA) following hot-pressing sintering(HPS). The MA was carried out in a high energy planetary ball milling with a speed of 350 rpm under Ar. And then milled powders were consolidated into disc of 40 mm in a diameter using HPS at the temperature of 1150°C for 2 h at the pressure of 50 MPa. Scanning electron microscopy (SEM, Zeiss Supra 55, Germany) with an energy dispersive spectrometer (EDS) was utilized to observe morphology of bulk alloys.

#### 2.2. The yield criterion and other model parameter

$$AJ_{2}' + BJ_{1}^{2} = \delta Y_{0}^{2} = Y_{\rho}^{2} \tag{1}$$

where  $J_2$  and  $J_1$  are the second invariant of the deviatoric stress tensor and the first invariant of the stress tensor respectively.  $Y_{\rho}$  is the yield stress of porous material;  $Y_0$  is the yield stress of non-porous material. A, B and  $\delta$  are function of relative density. Here the yield criterion of Shima-Oyane is applied as follows

$$F = \frac{1}{\gamma} \sqrt{\left(\frac{3}{2} \delta^d \delta^d + \frac{p^2}{\beta^2}\right)} - \delta_y \tag{2}$$

where  $\delta^d$  is the deviatoric stress tensor,  $\delta_y$  is the yield stress, P is hydrostatic pressure, and  $\gamma$ ,  $\beta$  are constant associated with relative density.

An experimental relationship between  $\nu$  and  $\rho$  has been proposed by Zhdanovich[10], which is assumed that

$$v = 0.5 \rho^{n} \tag{3}$$

here n = 2 when it comes to hot-pressing sintering.

In this study, the relationship between E and  $\theta$  (porosity) is as follows

$$E_{\theta} = E_0 (1 - \theta)^{3.4} \tag{4}$$

where  $E_{\theta}$  and  $E_{0}$  are corresponded with the elasticity modulus of non-porous material and porous material respectively.

The thermal properties of the powder vary with the porosity. The green body is considered as a special composite material in which the continuous phase is powder and the dispersed phase is considered a vacuum. Here thermal conductivity  $\lambda_0$  is generalized as

$$\lambda_{\rho} = \lambda_0 \frac{\rho}{1.5 - 0.5\rho} \tag{5}$$

where  $\lambda_{\rho}$  and  $\lambda_{0}$  are the thermal conductivity of porous material and non-porous material respectively.

### 2.3. Finite element simulation

The hot-pressing of HEA is regarded as a problem of nolinear large deformation contact, the model is transformed into a two dimensional plane strain, and the quadrilateral meshes are generated. The model is shown in Fig.1.

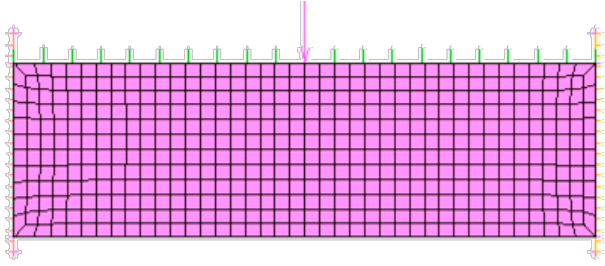


Fig. 1. The FEM model meshed by quadrilateral.

The above explicit constitutive model, yield criterion and other parameter were implemented to simulate the hotpressing process. In simulation, the diameter of cylindrical specimen is 40 mm with the height of 12 mm, the initial relative density was 0.5. Besides, the upper punch as well as the lower punch and die were considered as rigid bodies with no heat exchange throughout the sintering. And the other parameter according to former experiment were as follows.

Table 1. The thermophysical parameters of HEA in simulation.

Temperature(°C)	E (GPa)	- (MDa)	$\lambda_{\rho}\left(W/(m^{\circ}C)\right)$	Specific heat (J/(g°C))	Coefficient of thermal
		$\sigma_s$ (MPa)			expansion (10 <sup>-5</sup> /°C)

25	196	1600	15	0.52	1.6
600	157.56107	489	30	0.69	2.06
800	140.73119	183	31.5	0.75	2.27
1000	122.9932	48	34	0.84	2.8
1200	106.01646	15	36	0.9	3.1

# 3. Results and discussion

The results analyzed in this section are under the sintering parameter of 1150 °C and 50 MPa. Fig. 2 shows the distributions of stress during hot-pressing sintering varying with sintering time. The direction of X is along the radial and Y is along the axial which is the movement direction of punch. Before the temperature arrive to 1150°C, a pressure of 5MPa was imposed to prevent the powder from pumped away. Fig.2 (b) exhibits that the internal stress of material is 4.6MPa after heating for 3600 s, and the pressure forced to the punch is partially offset due to the friction from side wall. When simulating time is 6900 s, the pressure was added up to 50 MPa over 45 s, Fig. 2(c) shows the stress distribution of 6945 s, it is clear that the stress appear to 32 MPa, which is far away from the state of yield stress, and the material is in high temperature rheological state. The internal stress remained essentially constant with uniform distribution until the end of sintering, which is shown in Fig. 2(d).

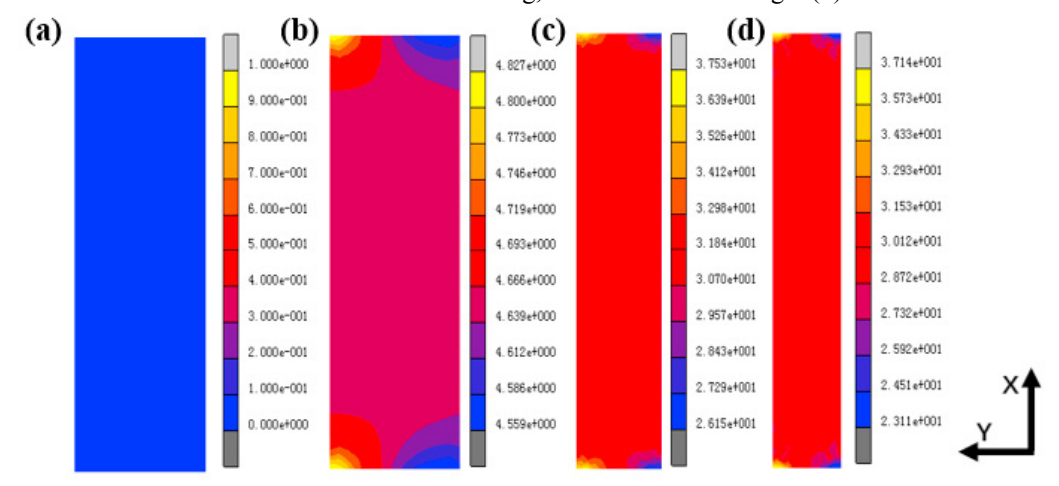


Fig. 2. The distribution of stress during hot-pressing sintering under different sintering time (a) 0s; (b) 3600s; (c) 6945s; (d) 14100s.

Fig.3 exhibits the distribution of relative density in process of sintering with the prolonging of time. Before the final pressure was forced, the compact has already possesses a certain degree of relative density except for the position close to the wall of mold, and it can be clearly seen from the Fig.3 (c). However, after 2 h of hot-pressing sintering, the relative density distribution appears uniform arriving to 96%.

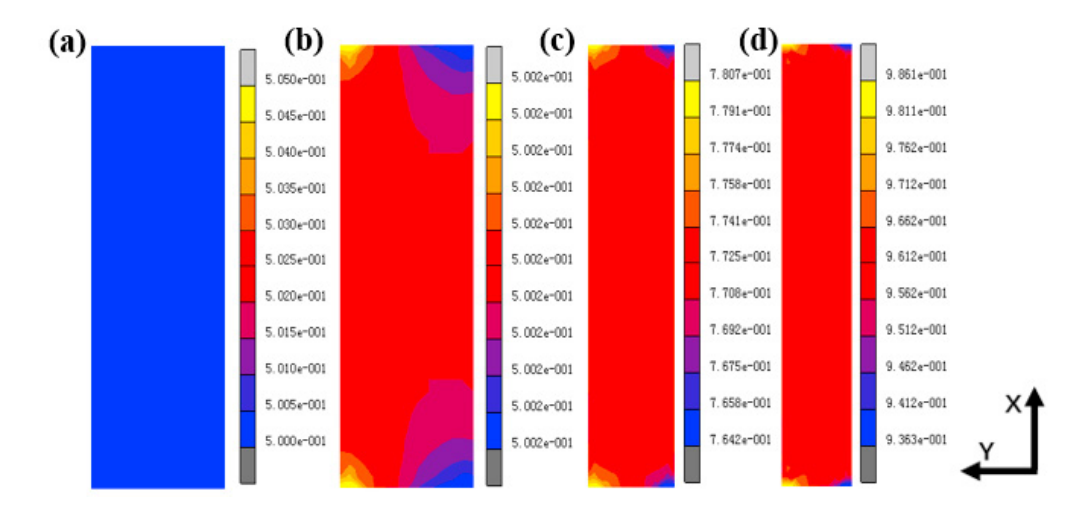


Fig. 3. The distribution of relative density during hot-pressing sintering under different sintering time (a) 0s; (b) 3600s; (c) 6945s; (d) 14100s.

Fig. 4 shows axial displacement and relative density of simulated compact varying with different temperature at the pressure of 50 MPa. It is clear that larger axial displacement is useful of improve the relative density of compact. A certain amount of displacement appeared at the pressure of 5MPa after 4500s, it indicates that softening occurred at high temperature. In the state of holding, the degree of sintering densification increased remarkably with the increasing of hot-pressing temperature. The relative density increased from 84.5% at 950 °C to 91.6% at 1050 °C, and reached 96.2% at 1150 °C under the condition of 50MPa for 2 h.

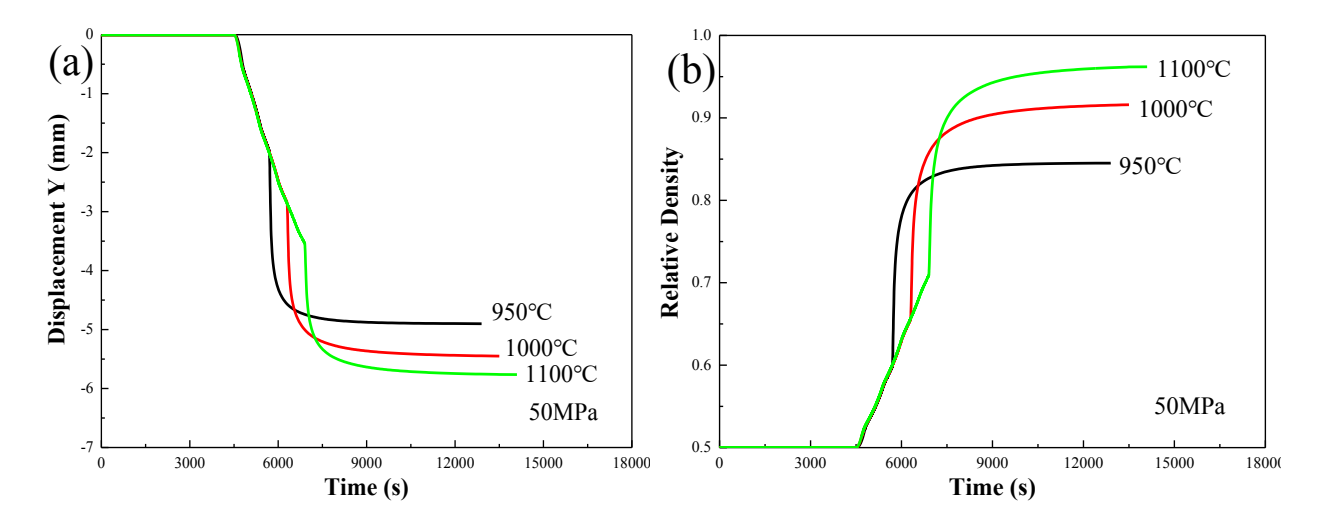


Fig. 4. (a) Axial displacement and (b) relative density of simulated compact at the pressure of 50 MPa in different temperature.

Fig.5 shows the axial displacement andrelative density of simulated compact at the temperature of 1150 °C in different pressure. It is clear that increasing pressure is in favor of improvement of relative density. However, the effect of increasing pressure on relative density is less obvious gradually, the density is increased by 7.8% when pressure increased from 10 MPa to 20 MPa, while the density can only be increased by 0.8% when pressure from 50 MPa to 60 MPa.

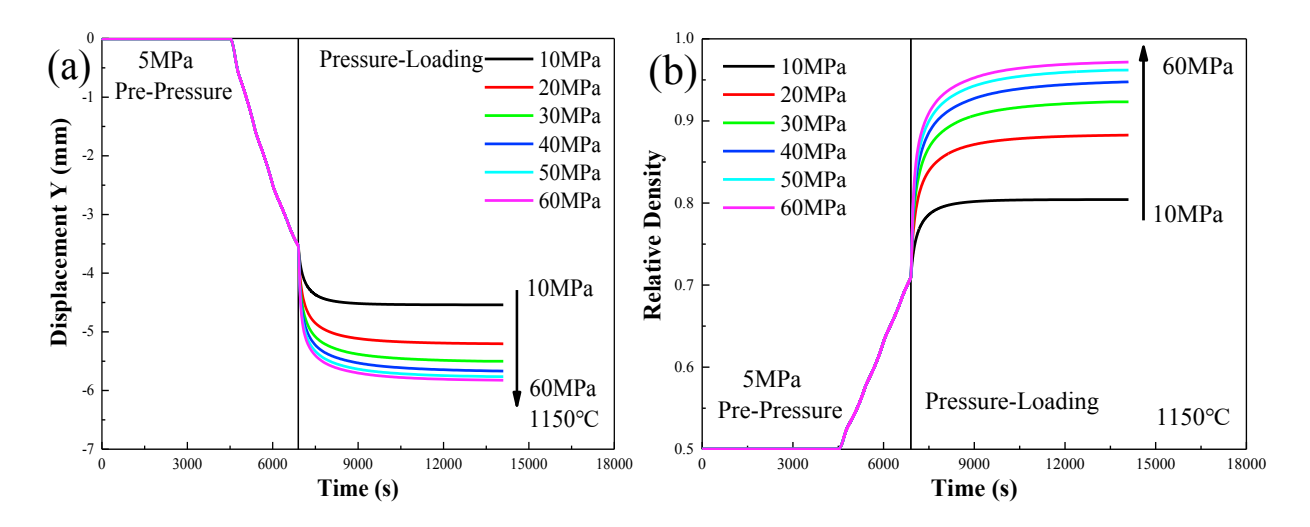


Fig. 5. (a) Axial displacement and (b) relative density of simulated compact at the temperature of 1150 °C in different pressure.

According to above results, the effect of temperature and pressure on relative density are shown in Fig.6. The relative density is improved with the increasing of temperature and pressure. The degree of densification reached 90% at 60MPa even if the temperature kept 950°C. However, it is difficult to diffuse evenly for HEA with the effect of sluggish diffusion, in such case, a higher sintering temperature is needed. Moreover, it is obvious that sintering at 50MPa and 1150°C, the compact achieve a densification of more than 95%, which can be used in the experiment.

Fig.7 exhibits the SEM micrographs together with EDS mapping of the bulk, it indicates that the chemical composition is getting uniform with no visible porosity.

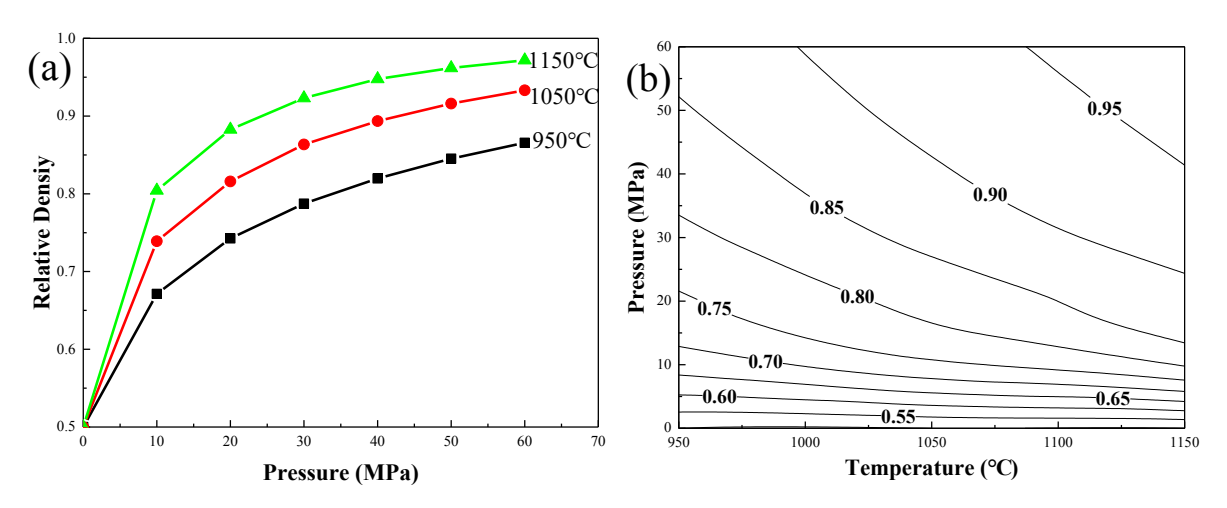


Fig. 6. The effect of temperature and pressure on relative density (a) the change of relative density along with pressure under the temperature of 950 °C, 1050 °C and 1150 °C respectively; (b) contour map of the effect of temperature and pressure on relative density.

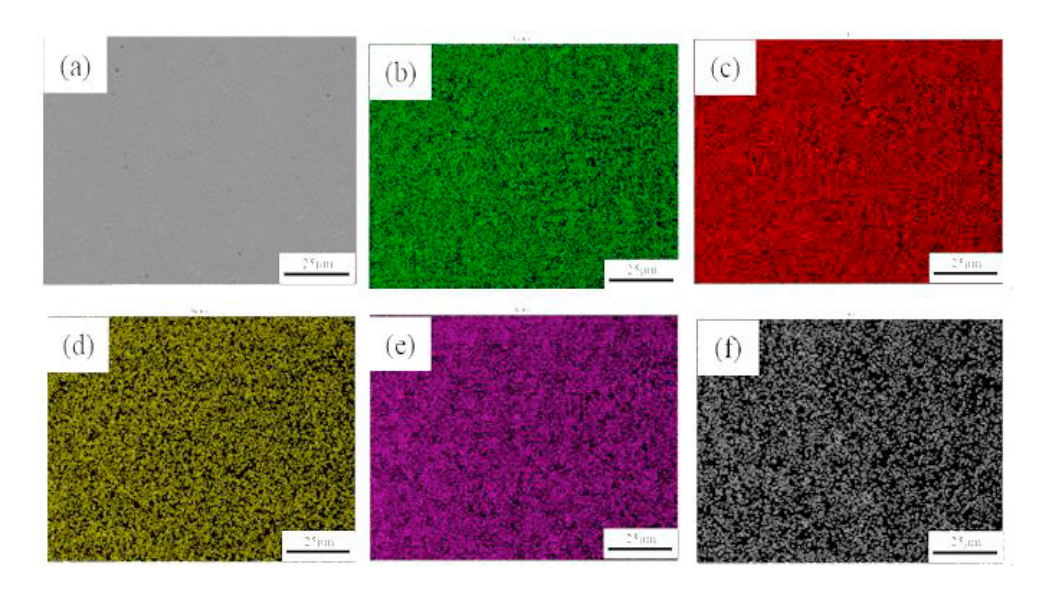


Fig. 7. The SEM images and corresponded to EDS results of element distribution (a)SEM image of sintered HEA; (b)~(f) element distribution of Fe, Cr, Ni, Al and Ti.

# 4. Conclusions

In the present work, finite element model based on elasto-plasticity for MA-powder sintering process has been implemented to analysis stress state and relative density distribution. The stress state together with relative density seem to be very well captured with the current numerical model over a wide variation temperature and pressure sintering process. The change law of relative density varying with temperature and pressure are obtained. After considering the influence of temperature and pressure on relative density synthetically, the relative density would reach 95% when the pressure and temperature is 40 MPa and 1150 °C respectively. The results of experiment indicates that the relative density of bulk HEA sintered at parameter of 50MPa and 1150 °C is over 95.15%, and the SEM images of the sintered HEA has no visible porosity, which is well agreement with the result according to FEM results. In conclusion, numerical modeling and simulation prove an effective approach to understand sintering HEA process and guide experiment.

# Acknowledgements

This work was supported by the National Natural Science Foundation of China [Grant Number 51401099]. The authors thank Yi Zhou, Ruiyang Li, Zhixuan Chen and Lianbo Luo for useful advice and discussion.

# References

- [1] Yeh J W, Chen S K, Lin S J, et al. Nanostructured High-Entropy Alloys with Multiple Principal Elements: Novel Alloy Design Concepts and Outcomes[J]. Advanced Engineering Materials, 2004,6(5):299-303.
- [2] Tsai M, Yeh J. High-Entropy Alloys: A Critical Review[J]. Materials Research Letters, 2014,2(3):107-123.
- [3] Chen R, Qin G, Zheng H, et al. Composition design of high entropy alloys using the valence electron concentration to balance strength and ductility[J]. Acta Materialia, 2018,144:129-137.
- [4] Chuang M, Tsai M, Wang W, et al. Microstructure and wear behavior of AlxCo1.5CrFeNi1.5Tiy high-entropy alloys[J]. Acta Materialia, 2011,59(16):6308-6317.
- [5] Ji W, Wang W, Wang H, et al. Alloying behavior and novel properties of CoCrFeNiMn high-entropy alloy fabricated by mechanical alloying and spark plasma sintering[J]. Intermetallics, 2015,56:24-27.
- [6] Ganji R S, Sai Karthik P, Bhanu Sankara Rao K, et al. Strengthening mechanisms in equiatomic ultrafine grained AlCoCrCuFeNi high-entropy alloy studied by micro- and nanoindentation methods[J]. Acta Materialia, 2017,125:58-68.

- [7] Oleszak D, Antolak-Dudka A, Kulik T. High entropy multicomponent WMoNbZrV alloy processed by mechanical alloying[J]. Materials Letters, 2018,232:160-162.
- [8] Diarra H, Mazel V, Boillon A, et al. Finite Element Method (FEM) modeling of the powder compaction of cosmetic products: Comparison between simulated and experimental results[J]. Powder Technology, 2012,224:233-240.
- [9] Biswas K. Comparison of various plasticity models for metal powder compaction processes[J]. Journal of Materials Processing Technology, 2005,166(1):107-115.
- [10] Zhdanovich G M, Sidorov V A, Yakubovskii C A. Distribution of pressure and density in powder compacts of complex configuration[J]. Soviet Powder Metallurgy and Metal Ceramics, 1982,21(5):369-372.